




Spontaneous generation of persistent activity in diffusively coupled cellular assembliesRia Ghosh ^{1,2} and Shakti N. Menon ¹¹*The Institute of Mathematical Sciences, CIT Campus, Taramani, Chennai 600113, India*²*Homi Bhabha National Institute, Anushaktinagar, Mumbai 400 094, India* (Received 27 September 2021; revised 29 December 2021; accepted 5 January 2022; published 21 January 2022)

The spontaneous generation of electrical activity underpins a number of essential physiological processes, and is observed even in tissues where specialized pacemaker cells have not been identified. The emergence of periodic oscillations in diffusively coupled assemblies of excitable and electrically passive cells (which are individually incapable of sustaining autonomous activity) has been suggested as a possible mechanism underlying such phenomena. In this paper we investigate the dynamics of such assemblies in more detail by considering simple motifs of coupled electrically active and passive cells. The resulting behavior encompasses a wide range of dynamical phenomena, including chaos. However, embedding such assemblies in a lattice yields spatiotemporal patterns that either correspond to a quiescent state or to partial or globally synchronized oscillations. The resulting reduction in dynamical complexity suggests an emergent simplicity in the collective dynamics of such large, spatially extended systems. Furthermore, we show that such patterns can be reproduced by a reduced model comprising only excitatory and oscillatory elements. Our results suggest a generalization of the mechanism by which periodic activity can emerge in a heterogeneous system comprising nonoscillatory elements by coupling them diffusively, provided their steady states in isolation are sufficiently dissimilar.

DOI: [10.1103/PhysRevE.105.014311](https://doi.org/10.1103/PhysRevE.105.014311)**I. INTRODUCTION**

Spontaneously recurring electrical activity is of crucial significance in a number of physiological contexts [1–3]. This is typically driven by pacemaker cells [4–6], such as the sinoatrial node in the heart, which comprises specialized cells that periodically generate signals initiating excitatory activity, leading to mechanical contraction [7]. However, such cells have not been observed in other contractile tissue, such as the myometrium of the gravid uterus [8]. It has been hypothesized that spontaneous activity in the latter contexts arises through interactions between electrically active and passive cells, local assemblies of which are capable of generating periodic waves of activation in the tissue through diffusive coupling [9,10]. These waves traveling through an organ are capable of sustaining spatiotemporally coherent contractions [11]. Indeed it has been demonstrated that one of the simplest ways to achieve this is by having an excitable cell coupled by gap junctions to one (or more) electrically passive cells characterized by a resting state membrane potential that is much higher than that of the excitable cell [12]. The coupling between these heterogeneous cell types causes the membrane potential of the excitable cell to be driven beyond its threshold, resulting in the generation of an action potential. Subsequently, the excitable cell attempts to return to its resting state, but after a period of recovery is again driven to exceed its threshold by the passive cells coupled to it, thereby resulting in a periodically recurring series of action potentials. Thus, although neither excitable nor passive cells are individually capable of spontaneous sustained activation, an assembly of these two cell types can generate periodic oscillations [13].

The emergence of periodic activity in a heterogeneous assembly of excitable and passive cells makes such a mechanism a viable candidate for self-organized system-wide coherent oscillations in physiological contexts where no pacemakers have been reported [14,15]. Indeed, it has been demonstrated that a lattice of excitable cells that are each coupled to a variable number of passive cells can exhibit a range of spatiotemporal phenomena consistent with those observed in the uterus during the transition to coherent activity seen prior to parturition [11,16,17]. However, noting that each local cellular assembly is either in an excitable or an oscillatory dynamical regime in isolation raises an important question: can the observed collective behavior be reproduced in an even simpler setting, viz., where each lattice site is occupied by either an oscillatory or an excitable element, a situation reminiscent of percolation [18]. In this paper, we consider the dynamics of two classes of systems, each capable of exhibiting spontaneous collective dynamics, one comprising electrically active and passive (EP) cells and the other comprising oscillatory and excitable (OE) cells. We observe that simple motifs of cells described using the EP model are capable of exhibiting a wide range of complex collective dynamical patterns. However, several of these are no longer observed when such cells are embedded in a spatially extended system, suggesting an emergent simplicity of the collective dynamics. More importantly, we observe that when cells described by the OE model are placed on a lattice, the resulting dynamics are qualitatively very similar to that obtained using the EP model. This points towards a more fundamental mechanism that could explain the emergence of spontaneous recurrent activity in physiologically relevant contexts.

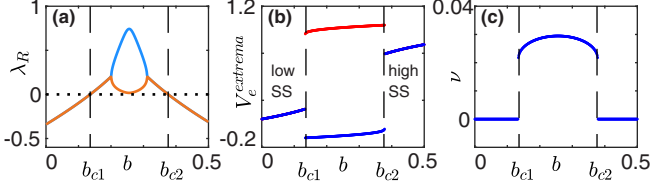


FIG. 1. Dependence of the dynamics of a single uncoupled FHN oscillator on the parameter b . (a) Real part of the eigenvalues (λ_R), obtained through a linear stability analysis, for a range of values of b . We find that λ_R crosses zero (horizontal broken line) at $b = b_{c1} (\simeq 0.136)$ and $b = b_{c2} (\simeq 0.376)$. (b) The system exhibits a low steady state (low SS) for $b < b_{c1}$ and a high steady state (high SS) for $b > b_{c2}$, as can be seen from the fact that the extrema of V_e (red and blue markers) coincide over these values of b . (c) In the range $b_{c1} < b < b_{c2}$, we observe oscillatory behavior, with the frequency ν exhibiting a maximum value at the center of this range. For reference, we display vertical dashed lines at $b = b_{c1}$ and $b = b_{c2}$ in each of the panels.

II. MODEL

To investigate in detail the range of complex behavior that emerges upon diffusively coupling excitable cells, each of which are in turn coupled to one or more passive cells, we consider the simplest possible assemblies of these cells capable of exhibiting spontaneous oscillatory activity. Following Ref. [11], we simulate the electrical activity of an excitable cell using the FitzHugh-Nagumo (FHN) model [19], which is capable of both excitable and oscillatory dynamics. The model describes the temporal evolution of an activation variable V_e (the membrane potential), and an inactivation variable g (an effective transmembrane conductance) as $\dot{V}_e = \mathcal{F}(V_e, g)$, $\dot{g} = \mathcal{G}(V_e, g)$. Here, $\mathcal{F}(V_e, g) = AV_e(V_e - \alpha)(1 - V_e) - g$ and $\mathcal{G}(V_e, g) = \epsilon(k_e V_e - g - b)$, where $A (= 3)$ and $k_e (= 1)$ govern the kinetics, $\alpha (= 0.2)$ is the excitation threshold and $\epsilon (= 0.08)$ is the recovery rate, while b provides a measure of the asymmetry of the limit cycle.

We observe that the real part of the eigenvalues (λ_R) of a single FHN unit, obtained from a linear stability analysis, is negative below a lower critical value $b_{c1} \simeq 0.136$ and above a higher critical value $b_{c2} \simeq 0.376$, indicating that the system does not oscillate for these ranges of b [Fig. 1(a)]. As seen in Fig. 1(b), the value of V_e in the resting state is close to 0 for $b < b_{c1}$ and is relatively large for $b > b_{c2}$. These regimes are hence referred to as low and high stable states, respectively. Furthermore, the system is capable of oscillatory behavior for $b_{c1} < b < b_{c2}$, as λ_R is positive in this range. The frequency of oscillations ν exhibits a maximum value at the midpoint $(b_{c1} + b_{c2})/2$ [Fig. 1(c)].

The temporal evolution of the passive cell is described in terms of its membrane potential V_p as $\dot{V}_p = K(V_p^R - V_p)$, where $V_p^R (= 1.5)$ is the resting state and $K (= 0.25)$ is the relaxation rate [20]. Each excitable cell is electrically coupled to $n_p (= 0, 1, 2, \dots)$ passive cells, where the conductance of the gap junctions between the two cell types is C_r . The set of equations used to describe the dynamics of an excitable cell i coupled to n_p^i passive cells, as well as to other excitable

cells j , is

$$\begin{aligned} \frac{dV_e^i}{dt} &= \mathcal{F}(V_e^i, g^i) + n_p^i C_r (V_p^i - V_e^i) + D \sum_{j \neq i} (V_e^j - V_e^i), \\ \frac{dg^i}{dt} &= \mathcal{G}(V_e^i, g^i), \\ \frac{dV_p^i}{dt} &= K(V_p^R - V_p^i) - C_r (V_p^i - V_e^i). \end{aligned} \quad (1)$$

The dynamics of an isolated excitable cell coupled to one or more passive cells depends on n_p and C_r . As V_p^R is much higher than the excitation threshold α , for a range of n_p and C_r the coupled excitable-passive system can exhibit oscillations. To demonstrate that such emergent oscillations result exclusively from the coupling we have chosen $b = 0$, so that in isolation the FHN dynamics converges to the low stable state. It is important to note in the context of the results reported here that when $C_r > 0.5$, oscillations are seen only for $n_p = 1$ while those excitable cells coupled to $n_p > 1$ passive cells converge to high stable states.

III. RESULTS

We first consider the simplest nontrivial assembly of dissimilar excitable-passive units, viz., a pair of excitable cells diffusively coupled with strength D , each interacting with a different number n_p of passive cells with strength C_r . The heterogeneity in n_p implies that the intrinsic behavior of the two units are dissimilar, and this can lead to a range of distinct collective dynamical patterns. The dynamical regimes obtained can be classified on the basis of the V_e time series of the excitable cells, using a set of order parameters with specified threshold values, as detailed in Fig. 2 and Ref. [21]: (i) oscillation death (OD), where both cells are in the same temporally invariant nonzero steady state; (ii) inhomogeneous steady state (ISS), where both cells are in different temporally invariant steady states; (iii) chimera (Ch), where only one of the two cells oscillate; (iv) inhomogeneous in-phase synchronization (IIS), where both cells oscillate in phase; (v) inhomogeneous out-of-phase synchronization (IOS), where both cells have the same frequency but are out of phase with each other, and, (vi) cluster synchronization (CS), where the two cells have different oscillation frequencies. The dynamical patterns obtained upon varying D and C_r are shown in Figs. 3(a)–3(d) for four distinct connection topologies of the assemblies (illustrated in the top right corners of the corresponding panels). The regions are identified according to the collective dynamics observed for the majority ($> 50\%$) of initial conditions. At low values of D , the two units can behave very differently, and we observe collective states such as Ch or CS. As D increases, the cells either become frequency locked or cease oscillating altogether. Note that the intrinsic heterogeneity of the two units prevents exact synchronization between them even for large D . For a given value of D , as C_r is decreased, eventually the cells stop oscillating (in isolation, neither an excitable nor a passive cell is capable of spontaneous activity). The qualitative nature of the collective dynamical patterns, in terms of (V_e, g) phase plane trajectories and individual time series, is displayed in Fig. 3(e).

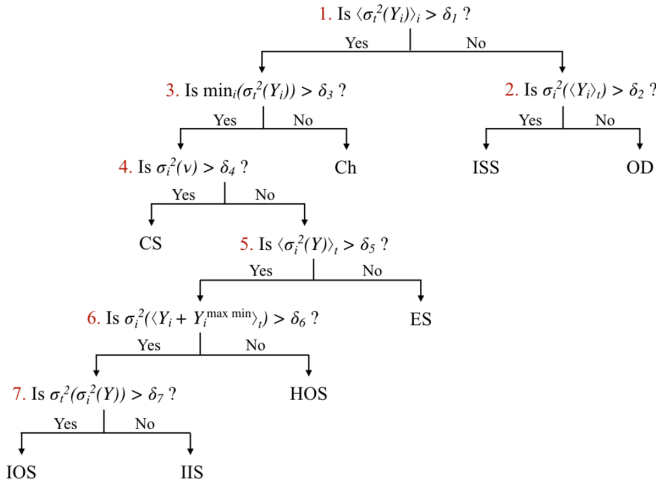


FIG. 2. Decision tree for identifying the dynamical state of a system of coupled excitable cells, each of which are connected to a variable number of passive cells (EP model). The order parameters used for determining the nature of the spatiotemporal pattern observed include the dispersions calculated across space [$\sigma_i^2(\cdot)$], or across time [$\sigma_i^2(\cdot)_t$], for the state variables Y_i ($i = 1, \dots, N$) or the oscillation frequencies ν . Averages calculated over space and over time are denoted by $\langle \cdot \rangle_i$ and $\langle \cdot \rangle_t$ respectively, while the deviation of the lowest value of the state variable for any node from its maximum calculated across space is denoted by $Y_i^{\max \min} = \max_i[\min_t(Y_i)] - \min_t(Y_i)$ [21]. The threshold values used to distinguish between the different states, viz., oscillation death (OD), inhomogeneous steady state (ISS), chimera (Ch), cluster synchronization (CS), exact synchronization (ES), homogeneous out-of-phase synchronization (HOS), inhomogeneous in-phase synchronization (IIS), and inhomogeneous out-of-phase synchronization (IOS), are: $\delta_1 = 10^{-3}$, $\delta_2 = 10^{-5}$, $\delta_3 = 10^{-3}$, $\delta_4 = 10^{-7}$, $\delta_5 = 10^{-5}$, $\delta_6 = 10^{-7}$, and $\delta_7 = 10^{-4}$.

In Figs. 3(f)–3(i), we display the variation of the frequency ν of the periodic activity exhibited by the excitable cells in the low D regime in each of the different assemblies (C_r is fixed at 0.25 in each case). We observe that an increase in D either gives rise to the cessation of oscillations [Fig. 3(f)] or a synchronized state in which the two units oscillate at a common frequency that is either lower [Fig. 3(g)], higher [Fig. 3(h)], or equal to [Fig. 3(i)] the higher of the pair of intrinsic frequencies (i.e., the frequencies of each unit at $D = 0$). We note that these results are qualitatively robust with respect to changes in V_p^R [21].

Just as coupling an excitable cell to one or more passive cells can, under appropriate conditions, give rise to oscillatory dynamics, we observe that spontaneous activity can arise upon coupling a pair of dissimilar units that do not oscillate in isolation. Figure 4(a) shows a pair of excitable cells, having $n_p = 0$ and $n_p = 2$, respectively, such that neither can independently oscillate for $C_r = 0.6$. However, upon increasing D sufficiently, we eventually observe a transition to a frequency synchronized state of the two units. We characterize this transition in terms of the eigenvalues obtained from a linear stability analysis. As seen in Fig. 4(b), we find that the real part of the eigenvalues λ_R are negative for small values of D , and that two of them change sign at $D \simeq 0.072$ [see inset

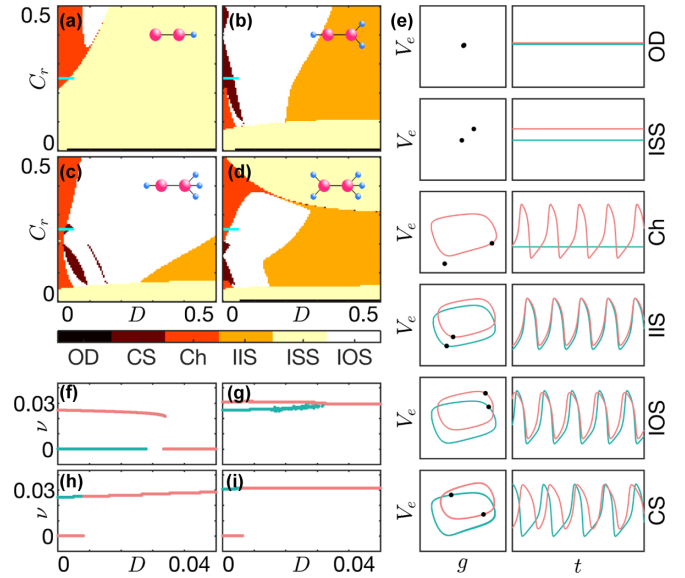


FIG. 3. Emergent dynamics obtained with different motifs of diffusively coupled excitable and passive cells. (a)–(d) Collective dynamical patterns observed over a range of values of coupling strengths D and C_r , obtained using different motifs (shown as insets in the corresponding panels, where the larger and smaller circles represent excitable and passive cells, respectively). The regimes are classified according to the dominant attractor obtained for the given parameter set [see Fig. 2]. (e) Qualitative nature of the patterns in (a)–(d), in terms of the phase plane trajectories and time series of the excitable cells [21]. The black dots represent the instantaneous position of the two cells on the corresponding limit cycle. (f)–(i) Variation of the frequency ν of the excitable cells on the left (green) and right (maroon) in each of the four motifs in (a)–(d) for $C_r = 0.25$, over the range of D indicated by horizontal cyan bars in (a)–(d). As D increases, the frequencies of the two cells merge, and for sufficiently strong coupling the system can either stop oscillating (f), or display a frequency that is between (g), greater than (h) or equal to (i) the maximum of the intrinsic frequencies.

of Fig. 4(b)]. This corresponds to the onset of oscillations, as can be seen in Fig. 4(c).

Upon increasing the number of units in an assembly, we observe that the system becomes capable of exhibiting more complex collective behavior including chaotic activity. However, a particularly intriguing collective state of coexisting chaotic and nonchaotic activity is observed in an assembly of three excitable cells, having $n_p = 1, 2, 3$, respectively, that are coupled in a chain [see top right corner of Fig. 5(a)]. For a large range of values of C_r and D , the system exhibits IOS [Fig. 5(a)]. However, in the CS regime, we observe a collective dynamical state that is characterized by chaotic behavior in the excitable cell with $n_p = 1$ with nonchaotic, periodic oscillations in the other two cells [Figs. 5(b)–5(d)]. The qualitative difference in the dynamics of the three excitable cells is evident upon comparing their time series [Fig. 5(b)], phase plane portraits [Fig. 5(c)], and power spectral densities [Fig. 5(d)]. A more rigorous comparison, considering the response of each cell to small perturbations, shows rapid divergence of the resulting trajectory from the unperturbed one for the chaotic unit, with no such deviation observed

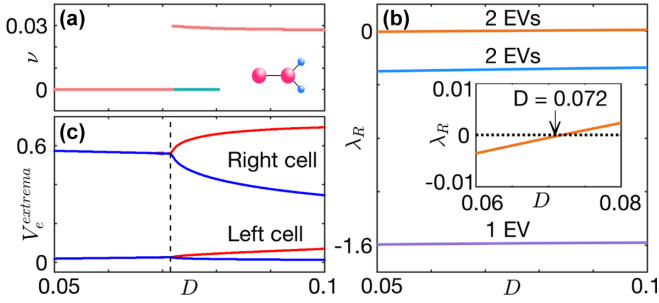


FIG. 4. Spontaneous emergence of oscillatory activity upon coupling a pair of quiescent units. (a) Variation of ν with D for $C_r = 0.6$, obtained using the motif shown as an inset, i.e., a pair of coupled excitable cells that are attached to zero and two passive cells, respectively. Although both cells are quiescent for low D , they exhibit oscillations for sufficiently large D . (b) Dependence of λ_R , corresponding to the real parts of the five eigenvalues of the system, on D . We note that two pairs of eigenvalues (EV) are complex conjugates and hence their real parts overlap, as indicated above the corresponding branches. The inset displays a zoomed-in segment of the panel, indicating the value of D at which two of the eigenvalues changes sign. (c) Bifurcation diagram of the extrema values of V_e for this system, showing the transition from a stable steady state to oscillations, where the maximum and minimum values for each of the two excitable cells are indicated by red and blue markers, respectively.

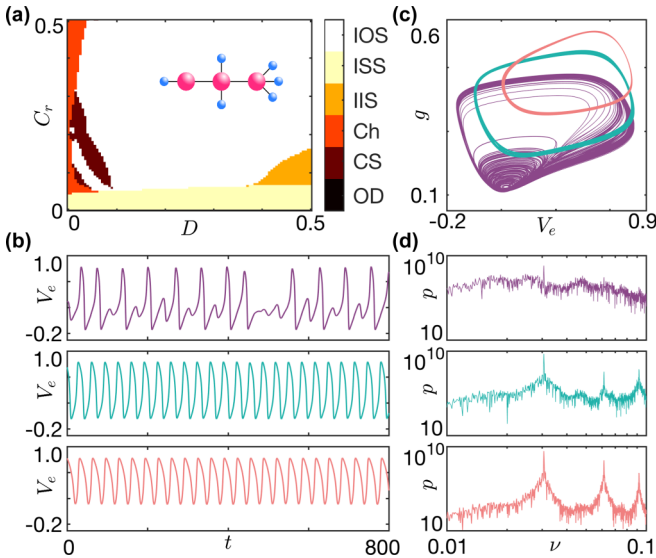


FIG. 5. Coexistence of chaotic and nonchaotic dynamical activity in a system comprising three diffusively coupled excitable cells, each connected to a different number (n_p) of passive cells. (a) Collective dynamical patterns observed over a range of values of diffusive coupling strengths D between excitable cells and the coupling C_r between excitable and passive cells for the system shown as an inset. The dynamical regimes are classified according to the dominant attractor obtained for the given parameter set, and are the same as those detailed in Figs. 3(a)–3(d). (b) Time series of membrane potential V_e of the excitable cells coupled to (top) $n_p = 1$, (middle) $n_p = 2$ and (bottom) $n_p = 3$ passive cells, for $D = 0.02$ and $C_r = 0.19$. (c)–(d) Phase plane trajectories and power spectral densities of the three excitable cells, colored as in the corresponding panels of (b).

for the other two units [21]. We note that permutations of the connection topology of this assembly, i.e., changing the order in which the cells with different values of n_p are placed in the chain, yields similar qualitative behavior, with chaotic dynamics consistently observed in the unit with the lowest n_p .

It may appear that increasing the size of the assemblies further, by adding more coupled excitable-passive units, can only lead to a further increase in the complexity of the collective dynamics. However, surprisingly, we observe an emergent simplicity in the behavior of large lattices of such units, with neighboring elements coupled diffusively to each other. Indeed, such an example is provided by a spatially extended model of uterine tissue, which is heterogeneous by nature, comprising electrically active myocytes that are excitable (thereby facilitating muscle contractions), as well as electrically passive cells such as interstitial Cajal-like cells (ICLC) [22] and fibroblasts [see top panel of Fig. 6(a)]. The system exhibits spontaneous oscillations for a range of values of C_r even though, in isolation, none of the individual cells are capable of autonomous periodic activity, as has been experimentally observed in uterine tissue [14,15]. More important from the perspective of the dynamical transition to periodic coordinated contraction of the myometrium, it is seen that increasing D results in the self-organized emergence of global synchronization, and eventually coherence [11,17]. It is striking that such coordination is achieved exclusively through local interactions between cells and does not require a centralized pacemaker such as that present in the heart (viz., the sinoatrial node).

The relative simplicity of the collective behavior of such a lattice of heterogeneous coupled cells can be shown by demonstrating that it can be captured by a reduced description of the system in terms of interacting dynamical elements, each of which are either in an oscillating or a steady state. In particular, we can replace excitable-passive cell assemblies that are capable of spontaneous periodic activation by a single FHN unit with $b_{c1} < b < b_{c2}$ (for concreteness, we choose $b_{osc} = 0.192$ for the simulations whose results are shown here), and FHN units with $b < b_{c1}$ ($> b_{c2}$) for cell assemblies exhibiting a low (high) stable state (we choose $b_{exc}^{low} = 0$ and $b_{exc}^{high} = 0.394$ for the simulations shown here). The resulting equivalent lattice now comprises only FHN units, a fraction f of which are in an oscillatory regime with the remaining being excitable by virtue of having different values of b [see Fig. 6(a), bottom panel]. Nevertheless, the system exhibits qualitatively identical behavior to that seen in models of uterine tissue simulated by coupling assemblies of excitable and passive elements, e.g., the occurrence of cluster synchronization at relatively low intercellular coupling that gives way to global synchronization of periodic activity (coordinated by propagating waves of excitation that traverse the lattice) for stronger coupling [Fig. 6(b)].

The similarity of the emergent properties of the simpler model can be established further by comparing the different dynamical regimes of the $f - D$ parameter space with that observed in the uterine model having heterogeneous cell types [11]. Indeed all the qualitatively distinct types of behavior reported in the latter can be seen in Fig. 6(c), including no oscillation (NO), with all cells in steady states; cluster

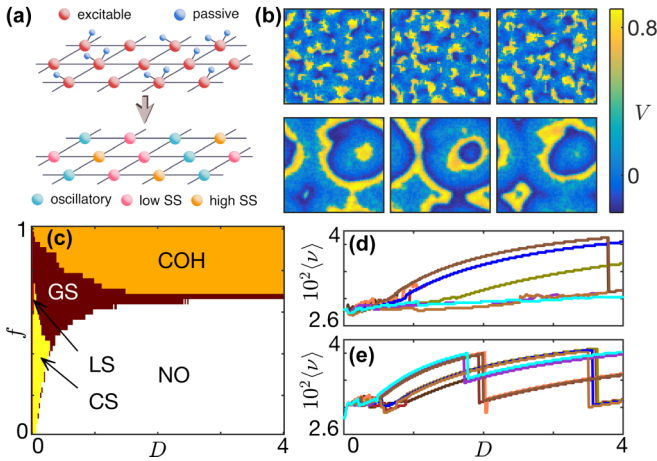


FIG. 6. Collective dynamics of a lattice of diffusively coupled elements that can be either excitable or oscillatory. (a) Schematic diagram of uterine tissue, modeled as a two-dimensional lattice where each site comprises an excitable cell coupled to n_p passive cells (top, the EP model), where the value of n_p at each site is drawn from a Poisson distribution. The dynamics at each site can equivalently be described through cells that are either oscillatory or excitable (bottom, the OE model). The latter cell type could be in one of two possible steady states (SS), characterized by low and high values of the state variable V . Note that the state of a cell in the bottom panel (high SS, low SS, or oscillatory) is chosen such that the uncoupled dynamics at that site is qualitatively the same as that of the corresponding site in the top panel. (b) Snapshots of the activity V in a planar simulation domain comprising an equal mixture of excitable and oscillatory elements ($f = 0.5$) diffusively coupled with strength D to nearest neighbors, showing (top row, $D = 0.1$) cluster synchronization (CS) and (bottom row, $D = 0.3$) global synchronization (GS). (c) Varying the diffusion coefficient D and the fraction of oscillatory cells f in the lattice for the case of the OE model, several distinct dynamical regimes are observed [see Fig. 7 for details]. (d)–(e) Variation of the mean oscillatory frequency $\langle \nu \rangle$ with D . Each curve is obtained by starting from different random initial states at low D and then gradually increasing D over time. In (d), the cell at each site can be either oscillatory (with probability $f = 0.7$) or excitable (with probability $1 - f$). In (e), we associate each lattice site with either an excitable or an oscillatory cell, following the procedure outlined in the main text. All simulations are performed on square lattices comprising 64×64 cells, with periodic boundary conditions.

synchronization (CS), marked by coexistence of multiple groups of cells, each characterized by a different frequency; local synchronization (LS), coexistence of quiescent cells with cells oscillating at a common frequency; global synchronization (GS), all cells have the same oscillation frequency; and coherence (COH), all cells exhibit phase synchrony. The decision tree used to classify these dynamical patterns is detailed in Fig. 7 and Ref. [21]. As in the EP model, the regions are identified according to the collective dynamics observed for the majority ($>50\%$) of initial conditions.

In the limit of large D , the lattice dynamics can be further simplified and an implicit analytical equation can be obtained for f_c , the fraction of FHN units that should be oscillatory for the system to exhibit persistent periodic excitations. It marks the boundary between the NO and COH regimes and is

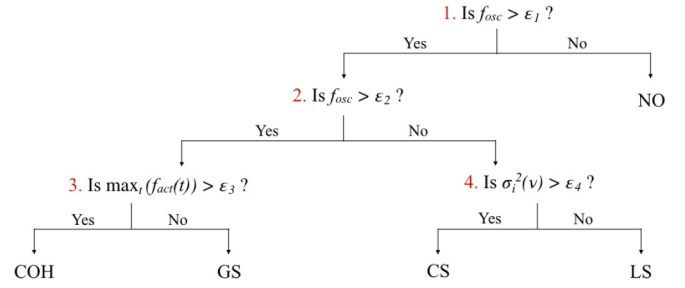


FIG. 7. Decision tree for identifying the dynamical state of a heterogeneous system of coupled cells, each of which can either be in the oscillatory or the excitable regime (OE model). The order parameters used for determining the nature of the spatiotemporal pattern observed include (i) f_{osc} : the number of oscillating nodes in the lattice, (ii) $\max_t [f_{act}(t)]$: the maximum number of nodes that were active (i.e., above the excitation threshold α) together over the period of observation, and (iii) $\sigma_f^2(\nu)$ is the dispersion of frequencies of all oscillating nodes calculated across space [21]. The threshold values used to distinguish between the states, viz., no oscillations (NO), cluster synchronization (CS), local synchronization (LS), global synchronization (GS), and coherence (COH), are $\epsilon_1 = 10^{-3}$, $\epsilon_2 = 0.999$, $\epsilon_3 = 0.995$, and $\epsilon_4 = 10^{-10}$.

given as $b_{c1} = (1 - f_c) b_{exc} + f_c b_{osc}$. For the situation shown in Fig. 6(c), $b_{exc} = b_{exc}^{low}$, which yields $f_c \sim 0.7$ upon inserting the corresponding numerical values.

We can investigate the collective dynamics around this asymptotic boundary between persistent oscillatory activity and a quiescent steady state by considering the case $f = 0.7$. In particular, we focus on the variation of the overall activation rate, measured by the mean frequency of periodic activation $\langle \nu \rangle$ (averaged over all oscillating elements in the lattice), as D is increased. In order to be consistent with the physiological setting, where the coupling between cells increases over the gestation period (as a result of hormone-induced increased expression of gap junctions that electrically couple the cells [23]), D is increased adiabatically over the course of a single realization, from a random initial condition at a low value of D . For the situation when $b_{exc} = b_{exc}^{low}$, shown in Fig. 6(d), $\langle \nu \rangle$ increases with D until it reaches a maximum value related to the reciprocal of the refractory period (set by the parameters of the FHN model). Increasing D further results in an abrupt drop in $\langle \nu \rangle$ as the number of propagating wavefronts in the system changes. A subsequent increase in D results in an increase in $\langle \nu \rangle$ generated by the new spatiotemporal pattern. This is qualitatively the same as the phenomenon observed for the model of uterine tissue involving assemblies of excitable and passive cells.

An even closer match between the two classes of models can be obtained if we replace each of the excitable elements with FHN elements having either $b_{exc} = b_{exc}^{low}$ or b_{exc}^{high} according to the following procedure: first, each lattice site is assigned a value n chosen from a Poisson distribution with mean $\lambda = f$. Note that this is identical to the process by which the number of passive cells (given by n) coupled to an excitable cell are determined in modeling uterine tissue with excitable-passive cell assemblies [11]. Next, FHN units in the oscillatory regime ($b = b_{osc}$) are placed at sites having $n = 1$, while FHN units with $b = b_{exc}^{low}$ (i.e., excitable element

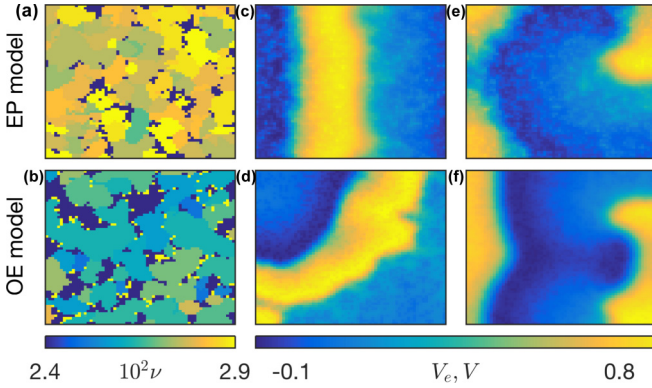


FIG. 8. Comparison of the spatiotemporal activity in two-dimensional lattices of cells described by the EP and OE models. We find that similar behavior can be seen for systems characterized by a large number of coupled units arranged in two-dimensional lattices, where each cell is described by the EP model (top row) or the OE model (bottom row). The two models can yield (a), (b) cluster synchronization, as evident from the spatial distribution of frequencies ν . In addition, both systems exhibit (c), (d) traveling wavefronts, and (e), (f) spiral waves, as can be seen from the instantaneous spatial distribution of V_e (top row) and V (bottom row), respectively.

with a low stable state) are placed at sites with $n = 0$. At sites having $n > 1$, corresponding to excitable-passive cell assemblies whose activity is arrested at a high stable state, FHN units with $b = b_{\text{exc}}^{\text{high}}$ are placed. Figure 6(e) shows the evolution of the mean frequency with D for $f = 0.7$ when the cellular coupling is increased adiabatically starting from a random initial condition over the course of a single realization. The resulting oscillatory-excitatory (OE) model can accurately reproduce dynamical behaviors reported for the model comprising excitable-passive (EP) cell assemblies [11]. These include the emergence of clusters characterized by a common oscillation frequency [Figs. 8(a), 8(b)], propagating wavefronts [Figs. 8(c), 8(d)], as well as self-sustained spiral waves in the GS regime [Figs. 8(e), 8(f)]. In addition, we observe that persistent periodic activity can arise upon coupling two FHN units that cannot independently oscillate, provided one of them is in the low and the other in the high stable state, a phenomenon analogous to the appearance of oscillations in assemblies of excitable and passive cells, which cannot sustain autonomous activity [21].

The qualitative equivalence of the collective behavior in large lattices for the two classes of models is all the more surprising as the dynamics of network motifs comprising excitable-passive cell assemblies (as seen in Figs. 3 and 5) is much more complex than that observed upon replacing each assembly by a FHN unit in the oscillatory or excitable regime. For instance, coupling a pair of EP cell assemblies, each of which oscillate at different frequencies, cannot give rise to exact synchronization even at large D . However, two FHN oscillators characterized by distinct b values (and hence, frequencies) can exhibit exact synchronization when coupled with sufficient strength. Furthermore, while we have reported motifs of connected EP cell assemblies that exhibit chimera

(Ch) regimes over a range of coupling strengths, such behavior cannot be seen in two coupled FHN oscillators with distinct intrinsic frequencies. We would also like to point out that nothing equivalent to the chaotic behavior observed in a motif comprising coupled EP cell assemblies (see Fig. 5) is seen in systems of coupled FHN oscillators arranged in a similar topology (viz., a chain comprising two oscillators having different intrinsic frequencies and an excitable element). Thus, even though the OE model reproduces the collective behavior of a large system of coupled EP cell assemblies, the dynamics at the microscopic level (i.e., motifs comprising only a few elements) can be extremely different for the two classes of models [21].

IV. CONCLUSION

To conclude, in this paper we have shown that while coupled excitable-passive cell assemblies are capable of exhibiting a wide range of dynamical behaviors including chaos, a macroscopic system comprising a large number of such elements diffusively coupled to their nearest neighbors on a lattice shows relatively simpler spatiotemporal phenomena. In particular, this resulting collective dynamics can be reproduced by a model comprising many elements, each described by a generic model for an excitable cell that is either in a steady state or in an oscillatory regime. Indeed, it suggests that the behavior associated with physiologically detailed models of uterine tissue activity [16,17,24] can be understood in terms of a reduced model involving a heterogeneous assembly of coupled oscillatory and excitable elements. More importantly, our results point towards a generalization of the mechanism proposed in Ref. [12] for the emergence of periodic activity in systems where none of the individual elements are intrinsically capable of oscillating. While it was shown there that persistent oscillations arise upon coupling excitable and electrically passive cells under certain circumstances, here we have shown that an oscillating system may emerge upon coupling elements, each of which are in isolation at time-invariant steady states, provided these states are dissimilar (i.e., the state variables associated with them have sufficiently distinct numerical values, corresponding to low and high). Furthermore, our demonstration of a large variety of dynamical attractors in small assemblies of excitable and passive elements can provide an understanding of the complex dynamics seen in electrically coupled heterogeneous subcellular compartments in neurons [25,26] and small networks of neurons interacting via gap junctions [27].

ACKNOWLEDGMENTS

We would like to thank Sitabhra Sinha and K. A. Chandrashekar for helpful discussions. S.N.M. has been supported by the IMSc Complex Systems Project (12th Plan), and the Center of Excellence in Complex Systems and Data Science, both funded by the Department of Atomic Energy, Government of India. The simulations and computations required for this work were supported by the Institute of Mathematical Sciences High Performance Computing facility (Nandadevi and Satpura clusters).

- [1] L. Glass, *Nature (London)* **410**, 277 (2001).
- [2] M. I. Rabinovich, P. Varona, A. I. Selverston, and H. D. I. Abarbanel, *Rev. Mod. Phys.* **78**, 1213 (2006).
- [3] S. Sinha and S. Sridhar, *Patterns in Excitable Media: Genesis, Dynamics, and Control* (CRC Press, Boca Raton, 2015).
- [4] J. D. Huizinga, L. Thuneberg, M. Klüppel, J. Malysz, H. B. Mikkelsen, and A. Bernstein, *Nature (London)* **373**, 347 (1995).
- [5] L. Thomson, T. L. Robinson, J. C. F. Lee, L. A. Faraway, M. J. G. Hughes, D. W. Andrews, and J. D. Huizinga, *Nature Med.* **4**, 848 (1998).
- [6] J. D. Huizinga *et al.*, *Nature Commun.* **5**, 3326 (2014).
- [7] M. R. Boyett, H. Honjo, and I. Kodama, *Cardiovasc. Res.* **47**, 658 (2000).
- [8] R. Smith, M. Imtiaz, D. Banney, J. W. Paul, and R. C. Young, *Am. J. Obstet. Gynecol.* **213**, 181 (2015).
- [9] J. H. E. Cartwright, *Phys. Rev. E* **62**, 1149 (2000).
- [10] C. D. Boschi, E. Louis, and G. Ortega, *Phys. Rev. E* **65**, 012901 (2001).
- [11] R. Singh, J. Xu, N. G. Garnier, A. Pumir, and S. Sinha, *Phys. Rev. Lett.* **108**, 068102 (2012).
- [12] V. Jacquemet, *Phys. Rev. E* **74**, 011908 (2006).
- [13] T. A. Quinn, P. Camelliti, E. A. Rog-Zielinska, U. Siedlecka, T. Poggioli, E. T. O'Toole, T. Knöpfel, and P. Kohl, *Proc. Natl. Acad. Sci. USA* **113**, 14852 (2016).
- [14] S. Wray, S. Kupittayanant, A. Shmygol, R. D. Smith, and T. Burdyga, *Exp. Physiol.* **86**, 239 (2001).
- [15] R. C. Young, *Best Pract. Res. Clin. Obstet. Gynaecol.* **52**, 68 (2018).
- [16] J. Xu, S. N. Menon, R. Singh, N. B. Garnier, S. Sinha, and A. Pumir, *PLoS One* **10**, e0118443 (2015).
- [17] J. Xu, R. Singh, N. B. Garnier, S. Sinha, and A. Pumir, *New J. Phys.* **15**, 093046 (2013).
- [18] D. Stauffer and A. Aharony, *Introduction to Percolation Theory* (CRC Press, Boca Raton, 1994).
- [19] J. Keener and J. Sneyd, *Mathematical Physiology* (Springer, New York, 1998).
- [20] P. Kohl, A. G. Kamkin, I. S. Kiseleva, and D. Noble, *Exp. Physiol.* **79**, 943 (1994).
- [21] See Supplemental Material at <http://link.aps.org/supplemental/10.1103/PhysRevE.105.014311> for simulation details and supporting figures.
- [22] R. A. Duquette, A. Shmygol, C. Vaillant, A. Mobasheri, M. Pope, T. Burdyga, and S. Wray, *Biol. Reprod.* **72**, 276 (2005).
- [23] E. Jahn, I. Classen-Linke, M. Kusche, H. M. Beier, O. Traub, R. Grummer, and E. Winterhager, *Hum. Reprod.* **10**, 2666 (1995).
- [24] W. C. Tong, C. Y. Choi, S. Karche, A. V. Holden, H. Zhang, and M. J. Taggart, *PLoS One* **6**, e18685 (2011).
- [25] B. V. Safronov, M. Wolff, and W. Vogel, *Biophys. J.* **78**, 2998 (2000).
- [26] J. M. Bekkers and M. Häusser, *Proc. Natl. Acad. Sci. USA* **104**, 11447 (2007).
- [27] G. J. Gutierrez, T. O'Leary, and E. Marder, *Neuron* **77**, 845 (2013).